Numerical study of the impact of artificial recharge through wells to control seawater intrusion in coastal aquifers

Philip Yousef K. Moussa(1), Asaad M. Armanuos(2) ,Noha Samir Donia(3), and Samah M. Morsy (4)

[1] Egyptian General Authority for Drainage Projects, Ministry of water resources and irrigation, Egypt, and Faculty of Graduate Studies and Environmental Research - Ain Shams University, Egypt [2] Irrigation and Hydraulics Engineering Department, Faculty of Engineering, Tanta university, Egypt .[3] Faculty of Graduate Studies and Environmental Research, Ain Shams University, Egypt . [4] Faculty of Science, Ain Shams University, Cairo, Egypt

ABSTRACT

The development of coastal regions is largely dependent on the groundwater system, which is the primary source of freshwater in these areas. Saltwater intrusion (SWI) into freshwater coastal aquifers is a widespread environmental concern that causes groundwater quality to deteriorate. This study investigates the impact of using artificial recharge through groundwater wells to control saltwater intrusion in unconfined coastal aquifers. The SEAWAT code was implemented to investigate the impact of injection of freshwater through groundwater wells to control saltwater intrusion in coastal aquifers. The semi-analytical of seawater wedge compared with the SEAWAT code solution for model verification. The artificial recharge tested for various depths of groundwater well, distances from the seaside, and artificial recharge rate. The points of artificial recharge located outside the saltwater intrusion wedge. The results confirmed that injection freshwater near to the toe of seawater intrusion achieved higher repulsion ratio. The maximum repulsion ration of seawater intrusion equal 18.2% achieved at point 7, which close to the sweater intrusion toe with injection ate equal 0.14 m^3/sec. Injection freshwater at points 7, 11, and 15 achieved the highest

repulsion ration for different values of injection rates. The minimum achieved repulsion ratio equals 5.8%, observed at point 1, which located far away from the point of toe. The findings of this research can be used to management of freshwater in groundwater systems in coastal aquifers.

Keywords: seawater intrusion, artificial recharge, repulsion ratio, groundwater aquifer, groundwater numerical model

Introduction

Because nearly 80% of the world's population lives in coastal regions and relies on regional aquifers for their freshwater, saltwater intrusion (SWI) is considered a major environmental issue (Barlow, 2000) (Ma et al., 2019). SWI poses a threat to groundwater systems in coastal areas. The key characteristics that induce changes in the status of coastal aquifers include groundwater pumping, climate change causes, rising sea levels, and changes in land use (Sebben et al., 2013).

Coastal aquifers are thought to be particularly sensitive to the SWI problem around the world (Aziz et al., 2019). The expansion of the SWI in these aquifers is being accelerated by rising sea levels. The Intergovernmental Panel on Climate Change (IPCC) has determined that the rise in sea level by the end of the century will be in the range of 0.52 to 0.98 meters (IPCC, 2013).

Various solutions for controlling or preventing SWI in coastal aquifers have been proposed (Todd, 1959, Van Dam, 1999, Oude Essink, 2001). The aquifer is artificially replenished with high-quality water (e.g., surface water, precipitation, extracted underground water, recycled water, or desalinated water) mostly within the positive or pressure barriers to retain the system's coastal gradient by raising the inland piezometric heads. Generally, artificial water recharge attempts to decrease flood flows, reserve freshwater in groundwater aquifers, maintain groundwater levels, reduce over-pumping, improve water quality, and reduce saline water bodies (Todd, 1959).

This methodology is one of the most popular, having been widely proposed and evaluated in the literature. Results of SWI numerical modeling in Australia's Burdekin and Delta aquifer (Narayan et al, 2007). (Mahesha & Nagaraja,1996) and Narayan et al. (Narayan, et al. 2003) illustrated that heavy pumping and decreased recharge rates contribute to the saltwater wedge's landward expansion. The following is a list of the more recent works, The saline wedge can be efficiently repelled by constant natural precipitation, according to a parametric analysis. (Mahesha, 1996a), (Mahesha, 1996b) suggested that groundwater recharge by injection wells is an effective strategy for delaying SWI in confined or unconfined aquifers with two or more distinct layers under any geological setting. The potential for deep recharge barriers to repel SWI has been investigated. (Luyun, 2011) using numerical, analytical, and experimental modeling. They came to the conclusion that implementing the recharging system farther and higher from the saltwater wedge's toe reduces its efficiency. Paniconi et al. (2001) quantitatively evaluated the methods. (Paniconi, et al., 2001), (Papadopoulou et al., 2005), (Narayan et al., 2007), and Allow (2012) applied for a variety of real-life case studies from around the world. Lu et al., (2013) analyzed the advantages of freshwater reinjection through a deep-well system placed between both the interface toe and the supply well.

SWI can be controlled by implementing a parallel injection–extraction system. By re-injecting some of the freshwater back into the coastal aquifer, the net freshwater extraction rate from the production well was boosted by up to 50% compared to cases without the injection well (single extraction well system), while also alleviating the SWI problem.

To manage SWI hazards, Sun and Semprich compared the effectiveness of freshwater injection to that of air injection. Despite the fact that deep air injection is less effective at creating an efficient pressure gradient against the intruded saltwater wedge, they found that depending on air injection (which is widely available) can be a good choice in locations where freshwater is scarce, (Sun & semprich, 2013). Surface ponds, lakes, canals, and other spreading recharge basins can also be utilized to replenish (only) unconfined aquifer systems by infiltrating collected water, (Abdalla & Al-Rawahi, 2013)

The impacts of a major dam (Al Khod dam) in the Sultanate of Oman on the decreasing of SWI were investigated. The dam was built with the intention of reducing underground water depletion during over-pumping seasons and collecting Wadi flows during heavy rainfall and runoff events. The recharge well was found to be effective and made a significant contribution to enhancing groundwater quality in the coastal zone, according to monitoring of the piezometric head and electrical conductivity measurements. (Yuansheng & Zhaohui, 2009) proposed artificial water recharge as a cost-effective way to control SWI and raise groundwater levels. They devised an integrated methodology for future sustainability of the flow system in the coastal city of Haihou, China, by delivering river water to interior lakes through a pre-constructed canal.

One of the primary constraints of recharge barriers employing desalinated water is the cost of providing high quality water (e.g., desalinated water) and its in-lieu delivery for recharging purposes. Furthermore, the lack of such water on a local level, particularly during dry years or in water-scarce areas, is a significant constraint. (Abd-Elhamid & Javadi, 2011). As a result, renewable water sources, such as treated wastewater, have received greater attention in recent years as sources of recharge for seawater intrusion reduction, (Hussain, et al., 2017). Reclaimed water used in common utility sectors or artificial storage in subsurface layers can help provide a portion of the water demand, withstand drought, and prevent attacks from SWI in coastal aquifers.

El-Arabi, (2012) introduced hydrogeological analysis and proposed scenarios for the Abu Rawash farm aquifer storage in order to assess the technical environmental. The environmental impact assessment (EIA) of artificial groundwater recharge was applied experiment to evaluate the feasibility standards for the coming recharge proposed projects. The results confirmed that groundwater artificial recharge for the aquifer utilizing the treated wastewater is considered promising technique while it requires additional detailed study to evaluate the aquifer characteristics affecting the mechanism of groundwater recharge with the treated wastewater.

(Abd-Elhamid & Abdelaty, 2017) utilized the SEAWAT code in order to simulate the seawater intrusion in the Nile Delta aquifer with concerning the saltwater intrusion control. Different proposed scenarios are applied for controlling seawater intrusion including freshwater recharge, brackish water abstraction, and a new approach (TRAD) is implemented for seawater intrusion in the Nile Delta aquifer. TRAD contains **T**reatment of wastewater and **R**echarge to the aquifer, **A**bstraction of brackish water, and **D**esalination. Comparing between the two proposed approaches and the novel method TRAD is introduced. The results of this study confirmed that all three proposed scenarios could be effective in seawater intrusion controlling; on the other hand utilizing the TRAD resulted in the maximum retreating of freshwater/saline water interface towards the Mediterranean Sea. TRAD is considered an effective technique to control seawater intrusion, is economically method, has minimum environmental impacts, and could be utilized for sustainable development of water resources in coastal areas.

Abd-Elhamid et al., (2022) investigated the land subsidence and expect the coming behavior of the middle Nile Delta aquifer. The (MODFLOW) numerical model is implemented to simulate the groundwater flow and an analytical solution to determine the land subsidence conditions. Three proposed scenarios are checked comprising; decreasing the Nile Delta aquifer recharge, increasing groundwater abstraction and combination between the two proposed scenarios. The results confirmed that reducing the recharge rate by 94.4%, 88.8%, and 83.2% resulted in to 30-, 60-, and 90-mm land subsidence, respectively, and while increasing the groundwater abstraction by 146%, 193%, and 233% resulted in land subsidence by 190, 380, and 560 mm, respectively, in the Nile delta. In addition, the combination between the two proposed scenarios resulted in 220-, 440-, and 650-mm land subsidence. The results confirmed that the future land subsidence due to over groundwater abstraction from the Nile Delta could be considered in the future development plans of the Egyptian country, which aim to raise the groundwater abstraction from the Nile Delta aquifer. Increasing the abstraction rate might raise the land subsidence that might cause many damages in different properties.

The main objective of this study is to investigate the effectiveness of using artificial recharge through wells to minimize and control seawater intrusion in coastal aquifer. The repulsion ratio of saltwater intrusion calculated for different runs to check the impact of the following parameters, wells depth, wells distances from seaside and groundwater artificial recharge rate.

Materials and Methods

For the simulations of SWI, the SEAWAT program has been intensively used. The finite difference SEAWAT code (Guo & Langevin, 2002) was implemented to model the effect of using artificial recharge to control seawater intrusion in unconfined coastal aquifers. SEAWAT is a code that links MODFLOW and MT3DMS together. The code is used to solve the linked groundwater flow and pollutant transport equations. SEAWAT uses groundwater flow simulations with varying density.

Figure 1. a shows the dimensions of the created model domain, which were 200m in horizontal and 100m in vertical coordinates. The cell size was adjusted at x = y = 0.50 cm. The saltwater head (h_s) in the saltwater boundary was set to equal 100 m. Freshwater and seawater densities were set to 1000 and 1025 kg/m^3, accordingly, with freshwater and seawater concentrations of 0.0 and 35,000 mg/L, respectively. The initial concentration of aquifer media was set to 0.0 mg/L. Assuming the aquifer was homogeneous and isotropic, the hydraulic conductivity value for the unconfined aquifer was 1 m/day in the x, y, and z directions. The porosity was adjusted to be 0.35. Table A1 presents the definitions of problem variables, and introduces the input variables of numerical simulations.

The SEAWAT model was run two times, first for the steady state case and secondly again for transient state. After the SWI wedge attained the steady state condition, injection through a recharge well was used. First, the model was run for the steady-state conditions. After reaching the steady state, injection the freshwater through injection wells were tested for five various recharge rates and for different fifteen locations of artificial recharge wells. By comparing the analytical solution of the saltwater wedge to the numerical one, the SEAWAT code was calibrated. The SWI simulation with the

artificial recharge well as a countermeasure was run for several sites of injection points positioned are outside the seawater intrusion wedge to determine the maximum repulsion ratio. The simulation was performed for various injection rates in order to achieve the greatest repulsion ratio value. The SWI repulsion ratio calculated with two reference values are the length of the seawater intrusion wedge and the area of the seawater intrusion wedge. For model calibration, the sweater intrusion wedge for semi analytical solution was compared by the results of SEAWAT code. Figure 1.b shows the comparison between the semi-analytical solution of Henery saltwater problem and the results of this study by SEAWAT code. The comparison showed a good agreement between the sweater intrusion wedges. The length of sweater intrusion wedge equals 99.5 m, and 97.9 m for semi-analytical solution and SEAWATE code respectively.

Table .1: Input data for Henry saltwater problem standard case with physical units according to Huyakorn et al., (1987)

Parameter	**Symbol**	**Value**
Aquifer length	L	200 m
Aquifer height	H	100 m
Saltwater density	ρ_s	1025kg/m^3
Freshwater density	ρ_f	1000 kg/m^3
Density difference	$\Delta\rho$	25 kg/m^3
Hydraulic conductivity	K	1 m/day
Porosity	φ	0.35
Diffusion coefficient	D	6.6x10^{-2} m^2.day
Longitudinal dispersivity	α_l	3.5 m
Transverse dispersivity	α_t	3.5 m
Freshwater inflow velocity	v	6.6x10^{-3} m/day
Artificial recharge rate	Q_r	0.06, 0.08, 0.10, 0.12, and 0.14 m^3/sec
Recharge well depth	Y_r	20, 40, 60, and 80m
Recharge well distance	X_r	80, 110, 140, 170 m

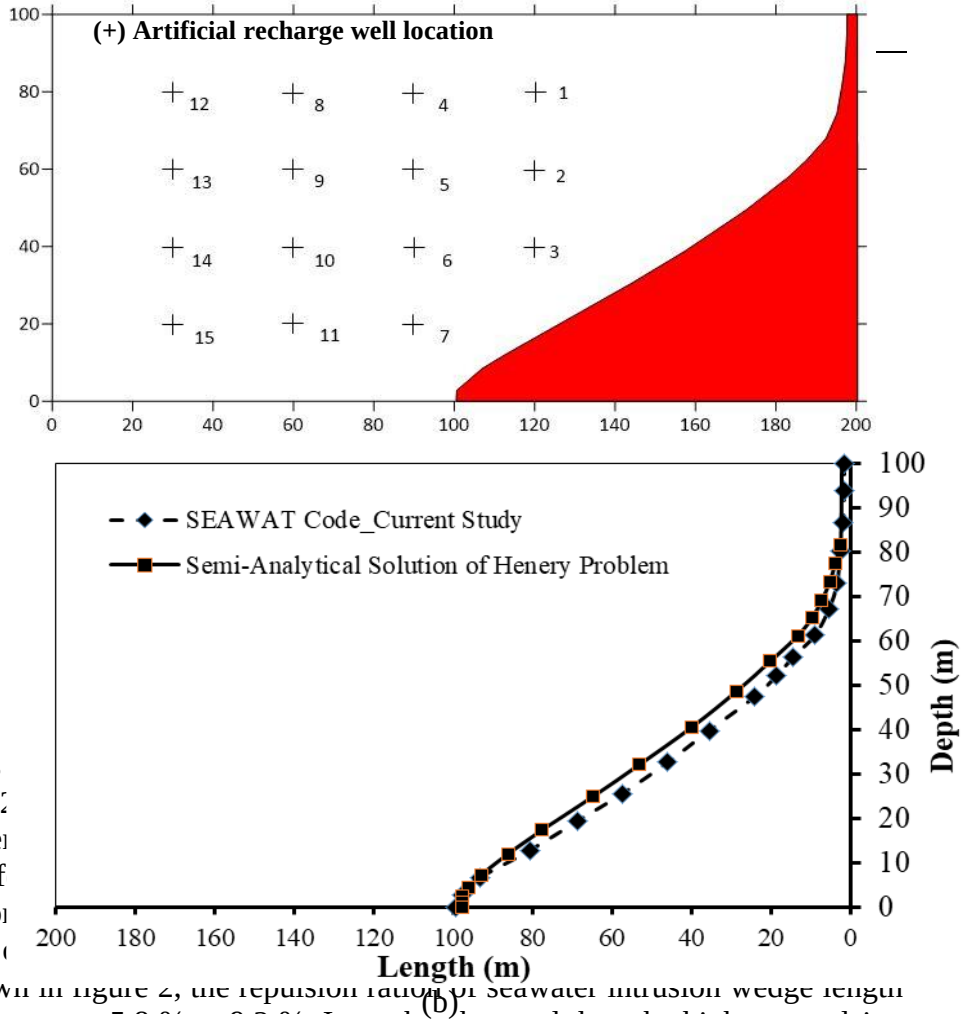

Results

Figure 7
seawater
m^3/sec f
state co
located

As shown in figure 2, the repulsion ratio of seawater intrusion wedge length

Figure .1: (a) Locations of fifteen artificial recharge points, ((+) the cross mark indicates the location of each artificial recharge well), (b) Comparison between seawater wedge for semi-analytical solution and SEAWAT code

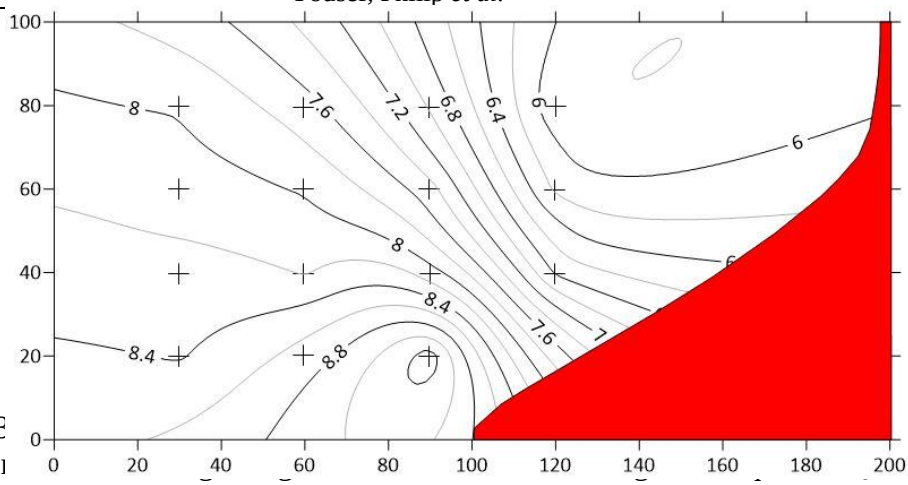

Figure .2: Contour lines of repulsion ratio of seawater intrusion for recharge rate Q_r= 0.06 m^3/sec for various fifteen points locations.

wedge length ranges from 5.7% to 11.8%. The maximum repulsion ratio was obtained with sites of artificial recharging situated close to the point of sweater infiltration wedge toe. At points 1 and 7, the minimum and maximum repulsion r

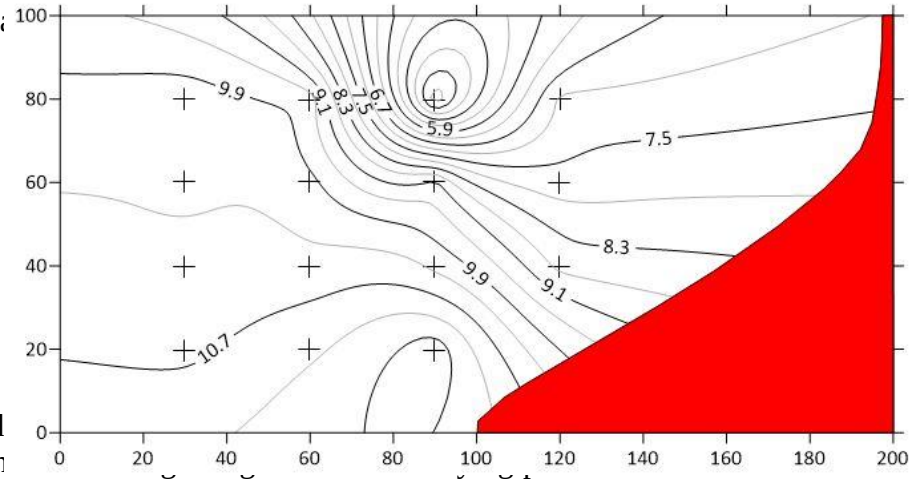

Figure .3: Contour lines of repulsion ratio of seawater intrusion for recharge rate Q_r= 0.08 m^3/sec for various fifteen points locations.

artificial recharge wells located outside the seawater intrusion zone. According to Figure 4, the repulsion ration of seawater incursion wedge length ranges from 7.7 to 14 percent. The highest repulsion ratio was observed with artificial recharge sites located around the point of sweater infiltration wedge toe. The minimum and highest repulsion ratios for points 1 and 7 were 7.7 percent and 14 percent, accordingly.

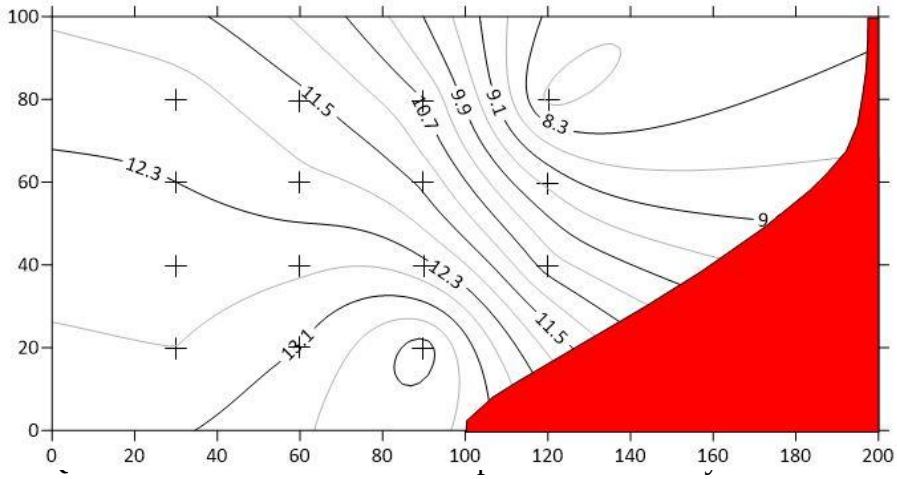

Figu ater
intr urge
rate n of

Figure .4: Contour lines of repulsion ratio of seawater intrusion for recharge rate Q_r= 0.10 m^3/sec for various fifteen points locations.

as shown in Figure 5. With artificial recharge sites situated near the point of saltwater intrusion wedge toe, the maximum repulsion ratio was observed. For points 1 and 11, the lowest and highest repulsion ratios were 10.4 percent and 15.2 percent, respectively.

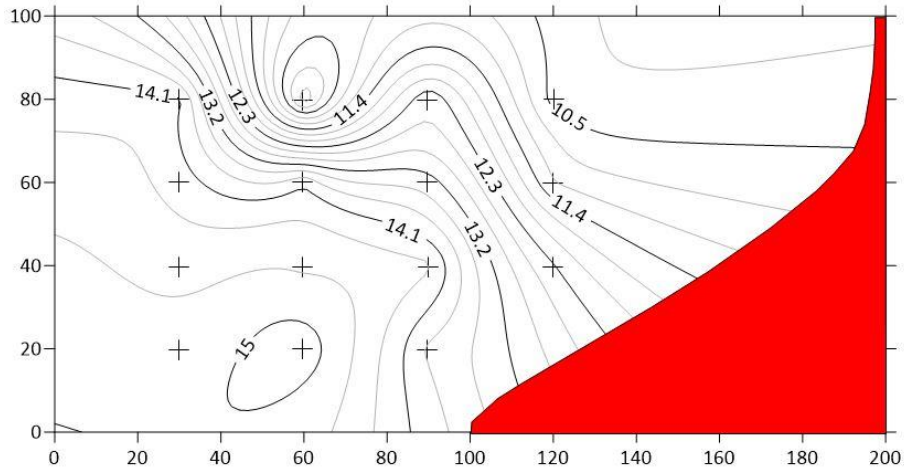

10

Figure .5: Contour lines of repulsion ratio of seawater intrusion for recharge rate Q_r= 0.12 m^3/sec for various fifteen points locations.

Figure 6 displays the contour line distribution for the repulsion ratio of saltwater intrusion wedge length at fifteen different places with an artificial recharge rate of Q_r= 0.14 m^3/sec. The color red indicates the steady-state condition of saltwater incursion. The positions of artificial recharge wells located outside the saltwater intrusion region are indicated by cross markings. Figure 6 depicts the repulsion ration of seawater intrusion wedge length, which ranges from 12 to 18.2 percent. The highest repulsion ratio was recorded at artificial recharge locations located near the point of saltwater intrusion wedge toe. The lowest and highest repulsion ratios for points 1 and 7 were 12 percent and 18.2 percent, respectively.

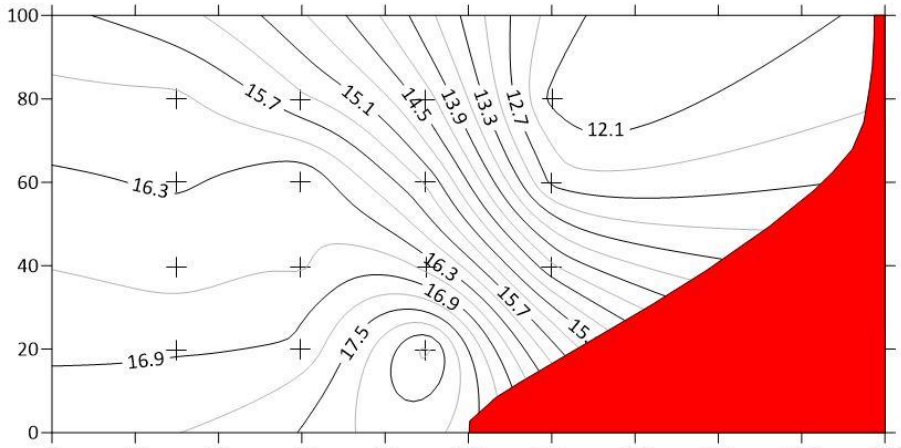

Table
seawa
achiev
recharge rates. The minimum repulsion ratio ranged from 5.7 to 12 % for

Figure .6: Contour lines of repulsion ratio of seawater intrusion for recharge rate Q_r= 0.14 m^3/sec for various fifteen points locations.

Table .1: Minimum and maximum achieved repulsion ratio for different proposed recharge rates scenarios

scenario	recharge rate Q_r	Minimum repulsion ratio	Point location	Maximum repulsion ratio	Point location
1	0.06	6 %	Point 1	9.2 %	Point 7

2	0.08	5.7 %	Point 4	11.8 %	Point 7
3	0.10	7.7 %	Point 1	14 %	Point 7
4	0.12	10.4 %	Point 1	15.2%	Point 11
5	0.14	12 %	Point 1	18.2 %	Point 7

Figures 7a and 7b show the retreat of the seawater intrusion wedge for various artificial recharge rates are 0.06, 0.08, 0.10, 0.12, and 0.14 m^3/sec for points 1 and 2 respectively. The seawater intrusion wedge retreated to seaside by increasing the artificial recharge rates through well from 0.06 to 0.14 m^3/sec. As shown in figure 7a, the seawater intrusion wedge length attenuated from 99 m at steady state condition to 93.50, 91.90, 90.20, 88.90, and 87.40 m for recharge rates equal 0.06, 0.08, 0.10, 0.12, and 0.14 m^3/sec respectively. Furthermore, the achieved repulsion ratio reached 5.85% and 12.02% for artificial recharge rate equal 0.06, and 0.14 m^3/sec respectively. In addition, as presented in figure 7b, the seawater intrusion wedge length attenuated from 99 m at steady state condition to 93.20, 91.40, 90.10, 88.20, and 86.60 m for recharge rates equal 0.06, 0.08, 0.10, 0.12, and 0.14 m^3/sec respectively. Furthermore, the achieved repulsion ratio reached 6.16% and 12.62% for artificial recharge rate equal 0.06, and 0.14 m^3/sec respectively.

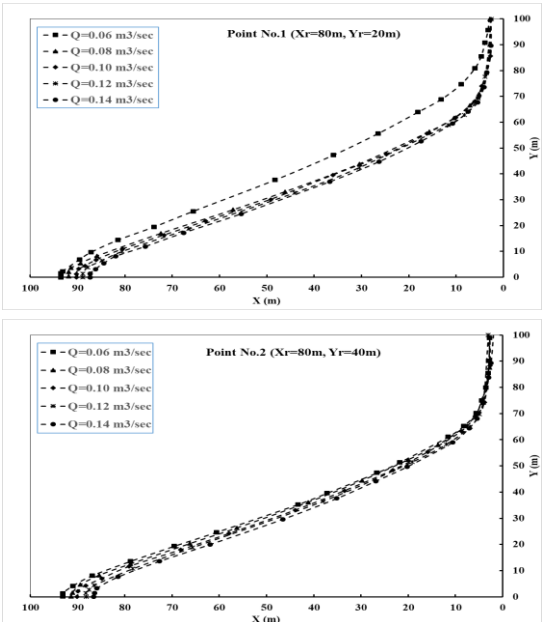

Figures 8a and 8b depict the retreat of the saltwater intrusion wedge for various artificial recharge rates of 0.06, 0.08, 0.10, 0.12, and 0.14 m^3/sec for locations 3 and 4. By raising the artificial recharge rates through the well from 0.06 to 0.14 m^3/sec, the seawater intrusion wedge receded to the seaside. The saltwater intrusion wedge length decreased from 99 m in steady state to 90.6, 88.6, 86.9, 85.3, and 86.7 m for recharge rates of 0.06, 0.08, 0.10, 0.12, and 0.14 m^3/sec, as shown in figure 8a. Additionally, with artificial recharge rates of 0.06 and 0.14 m^3/sec, the achieved repulsion ratio was 6.76 percent and 14.24 percent, respectively.

Furthermore, as shown in figure 8b, the seawater intrusion wedge length decreased from 99 m at steady state to 92, 95.4, 88.5, 86.8, and 84.90 m for recharge rates of 0.06, 0.08, 0.10, 0.12, and 0.14 m^3/sec. Moreover, with artificial recharge rates of 0.06 and 0.14 m^3/sec, respectively, the achieved repulsion ratio was 6.96 percent and 14.34 percent.

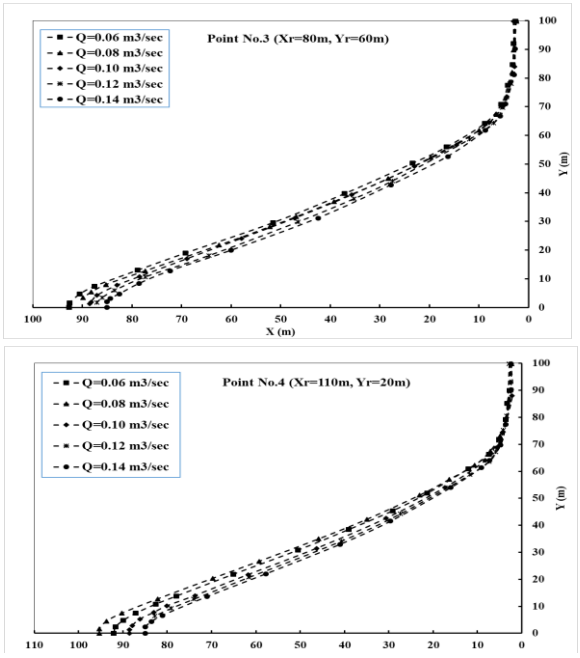

Figure 8: Salt water intrusion wedge for five different

Figures 9a and 9b show the retreat of the seawater intrusion wedge at different artificial recharge rates of 0.06, 0.08, 0.10, 0.12, and 0.14 m^3/sec for locations 5 and 6. The saltwater intrusion wedge withdrew to the sea side by increasing the artificial recharge rates through the well from 0.06 to 0.14 m^3/sec. Figure 8a shows that the seawater intrusion wedge length dropped from 99 m in steady state to 92.2, 90.05, 87.8, 86.2, and 84.1 m for recharge rates of 0.06, 0.08, 0.10, 0.12, and 0.14 m^3/sec. Furthermore, at artificial recharge rates of 0.06 and 0.14 m^3/sec, respectively, the achieved repulsion ratio was 7.47 percent and 15.35 percent. Furthermore, the saltwater intrusion wedge length dropped from 99 m at steady state to 91.4, 89.1, 86.9, 84.9, and 82.90 m for recharge rates of 0.06, 0.08, 0.10, 0.12, and 0.14 m^3/sec, as shown in figure 9b. Furthermore, using artificial recharge rates of 0.06 and 0.14 m^3/sec, the achieved repulsion ratio was 8.07 percent and 16.46 percent, respectively.

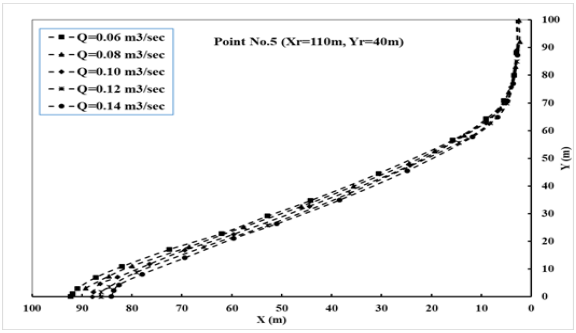

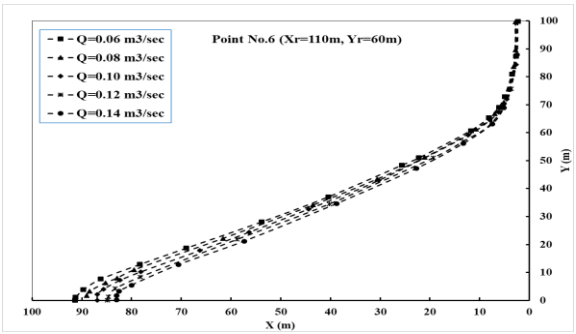

Figure 9: Salt water intrusion wedge for five different recharge

Figures 10a and 10b depict the retreat of the saltwater intrusion wedge for locations 7 and 8 at various artificial recharge rates of 0.06, 0.08, 0.10, 0.12, and 0.14 m^3/sec. By raising the artificial recharge rates through the well from 0.06 to 0.14 m^3/sec, the seawater intrusion wedge retreated to the sea side. Figure 10a indicates that for recharge rates of 0.06, 0.08, 0.10, 0.12, and 0.14 m^3/sec, the seawater intrusion wedge length decreased from 99 m in steady state to 90.1, 87.6, 85.2, 83.2, and 80.9 m. Furthermore, the obtained repulsion ratio was 9.29 percent and 18.48 percent at artificial recharge rates of 0.06 and 0.14 m^3/sec, accordingly. Moreover, as shown in figure 10b, the seawater intrusion wedge length decreased from 99 m in steady state to 91.5, 89.6, 87.7, 85.5, and 83.8 m for recharge rates of 0.06, 0.08, 0.10, 0.12, and 0.14 m^3/sec. Additionally, using artificial recharge rates of 0.06 and 0.14 m^3/sec, the repulsion ratio attained was 7.67 percent and 15.45 percent, accordingly.

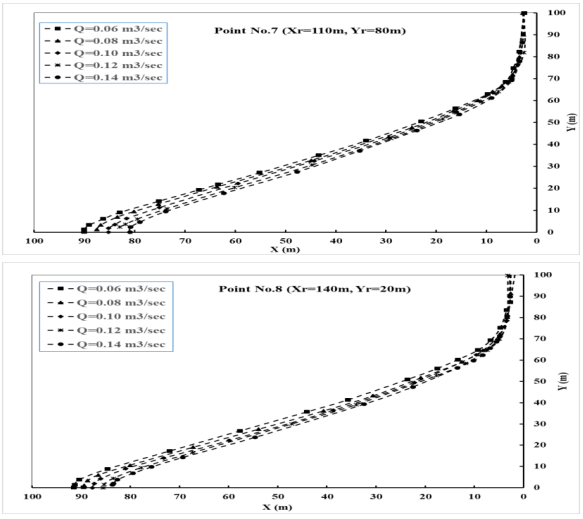

Figures 11a and 11b show the retreat of the seawater intrusion wedge at various artificial recharge rates of 0.06, 0.08, 0.10, 0.12, and 0.14 m^3/sec for positions 9 and 10. The saltwater intrusion wedge receded to the sea side by increasing the artificial recharge rates through the well from 0.06 to 0.14 m^3/sec. Figure 11a shows that the saltwater intrusion wedge length reduced from 99 m in steady state to 91.4, 89.2, 87.2, 85.2, and 83.3 m for recharge rates of 0.06, 0.08, 0.10, 0.12, and 0.14 m^3/sec. Moreover, for artificial recharge rates of 0.06 and 0.14 m^3/sec, the obtained repulsion ratio was 7.97 percent and 15.95 percent, respectively. Furthermore, as shown in figure 11b, the steady-state length of the saltwater intrusion wedge dropped from 99 m to 91, 88.7, 86.7, 84.8, and 82.9 m for recharge rates of 0.06, 0.08, 0.10, 0.12, and 0.14 m^3/sec. Furthermore, for artificial recharge rates of 0.06 and 0.14 m^3/sec, the repulsion ratio was 8.16 percent and 16.56 percent, respectively.

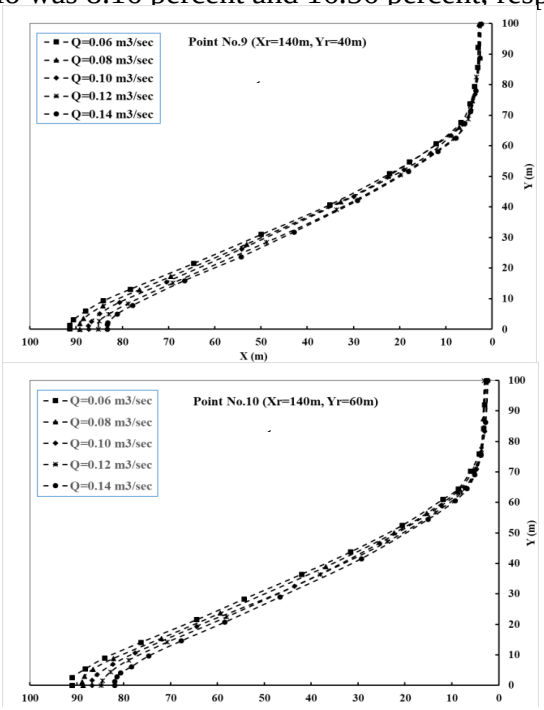

Figure 11: Saltwater intrusion wedge for five different

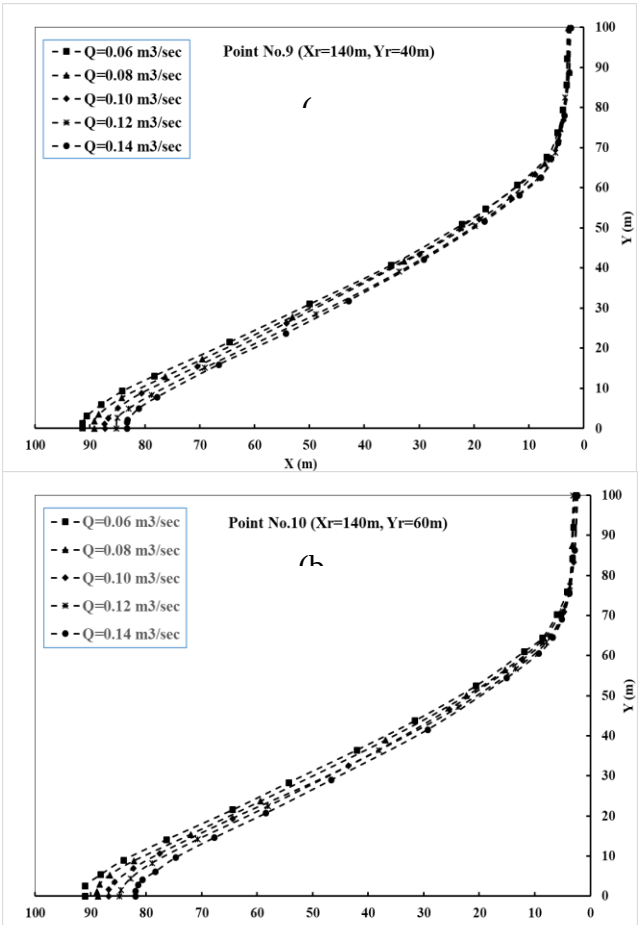

Figure .11: Saltwater intrusion wedge for five different recharge rates for

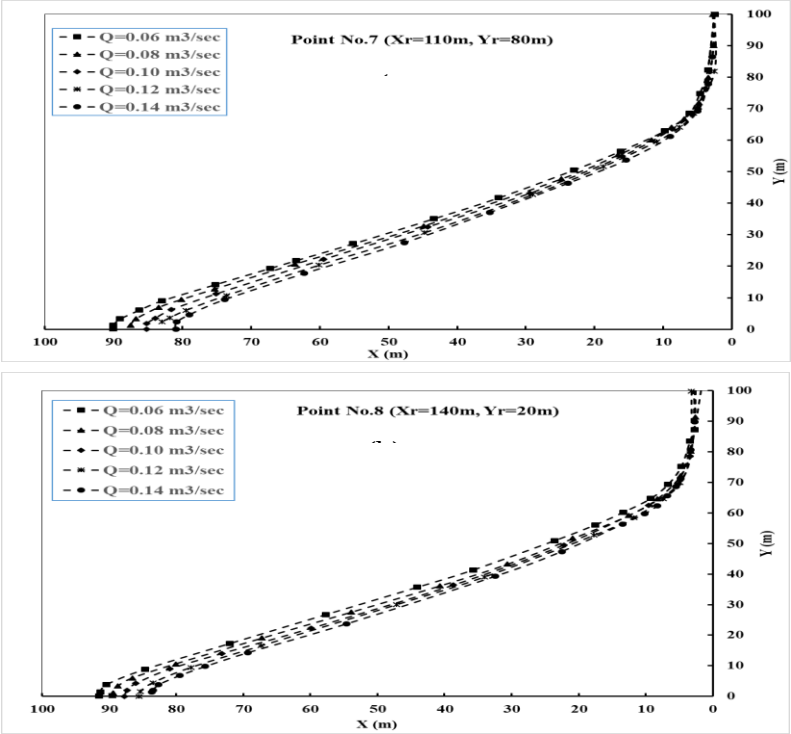

Figure 10: Saltwater intrusion wedge for five different recharge rates for points

Figures 12a and 12b depict the retreat of the saltwater intrusion wedge for positions 11 and 12 at varied artificial recharge rates of 0.06, 0.08, 0.10, 0.12, and 0.14 m^3/sec. By raising the artificial recharge rates through the well from 0.06 to 0.14 m^3/sec, the seawater intrusion wedge withdrew to the sea side. Figure 12a indicates that for recharge rates of 0.06, 0.08, 0.10, 0.12, and 0.14 m^3/sec, the seawater intrusion wedge length decreased from 99 m in steady state to 90.4, 88.2, 86, 84, and 81.9 m. Furthermore, the repulsion ratio observed for artificial recharge rates of 0.06 and 0.14 m^3/sec was 8.68 percent and 16.96 percent, accordingly. Additionally, as shown in figure 12b, with recharge rates of 0.06, 0.08, 0.10, 0.12, and 0.14 m^3/sec, the steady-state length of the saltwater intrusion wedge decreased from 99 m to 91.4, 89.2,

87.0, 85.2, and 83.30 m. Moreover, the repulsion ratio was 7.97 percent and 16.06 percent for artificial recharge rates of 0.06 and 0.14 m^3/sec, accordingly.

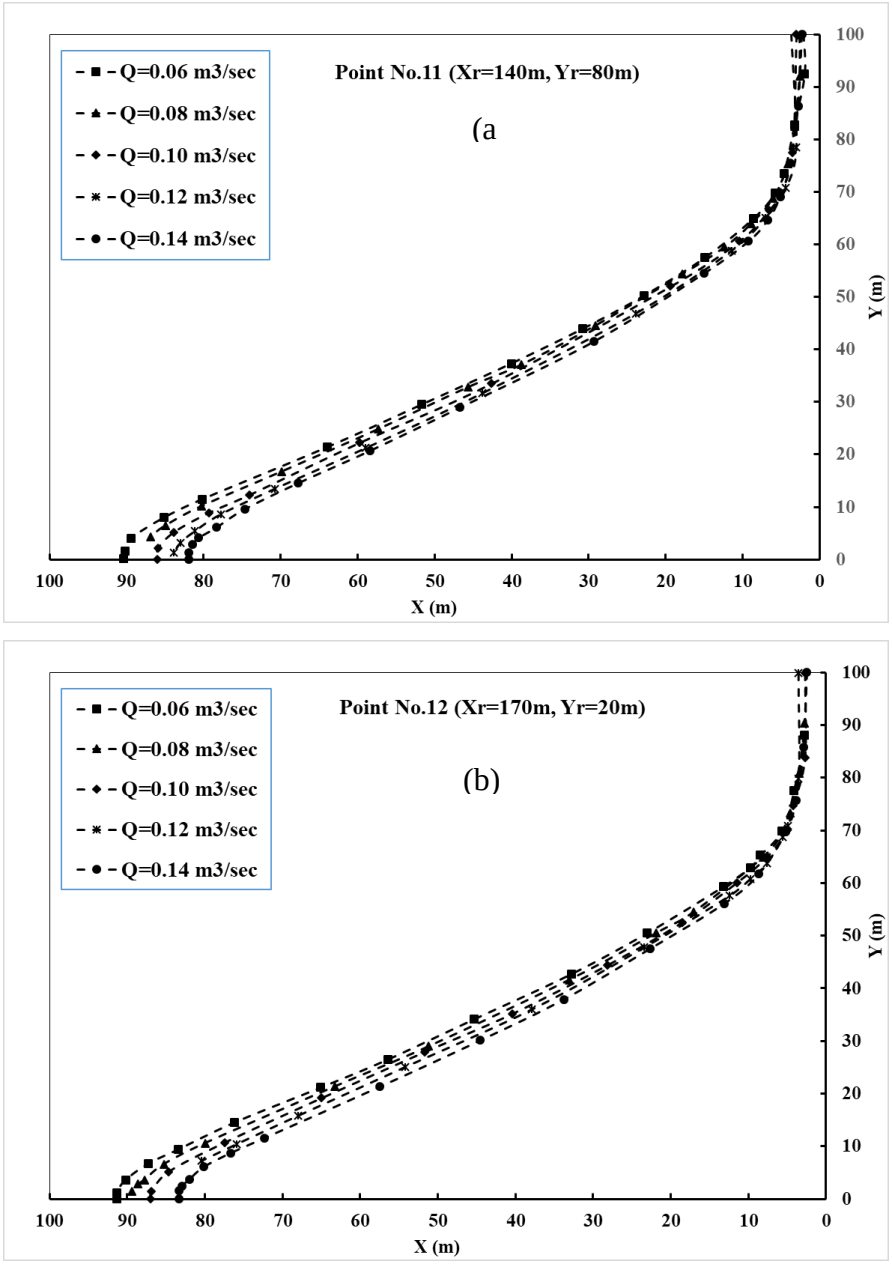

Figure .12: Saltwater intrusion wedge for five different recharge rates for points number:(a) 11 and (b) 12

Figures 13a, 13b and 13c show the retreat of the saltwater intrusion wedge at various artificial recharge rates of 0.06, 0.08, 0.10, 0.12, and 0.14 m^3/sec for locations 13, 14, and 15. The saltwater intrusion wedge retreated to the sea side by increasing the artificial recharge rates through the well from 0.06 to 0.14 m^3/sec. Figure 13a shows that the saltwater intrusion wedge length reduced from 99 m in steady state to 91.2, 89.10, 87.0, 85.0, and 83.3 m for recharge rates of 0.06, 0.08, 0.10, 0.12, and 0.14 m^3/sec. Furthermore, with artificial recharge rates of 0.06 and 0.14 m^3/sec, the repulsion ratio was 8.08 percent and 16.26 percent, respectively.

Furthermore, with recharge rates of 0.06, 0.08, 0.10, 0.12, and 0.14 m^3/sec, the steady-state length of the saltwater intrusion wedge dropped from 99 m to 92.4, 90.02, 88.9, 86, and 82.80 m, as seen in figure 13b. Additionally, with fake recharge rates of 0.06 and 0.14 m^3/sec, the repulsion ratio was 8.38 percent and 16.46 percent, respectively.

Furthermore, figure 13c indicates that for recharge rates of 0.06, 0.08, 0.10, 0.12, and 0.14 m^3/sec, the saltwater intrusion wedge length decreased from 99 m in steady state to 90.0, 88.7.05, 86.7, 88.9, and 82.6 m. Additionally, the repulsion ratio was 8.38 percent and 16.86 percent with artificial recharge rates of 0.06 and 0.14 m^3/sec, accordingly.

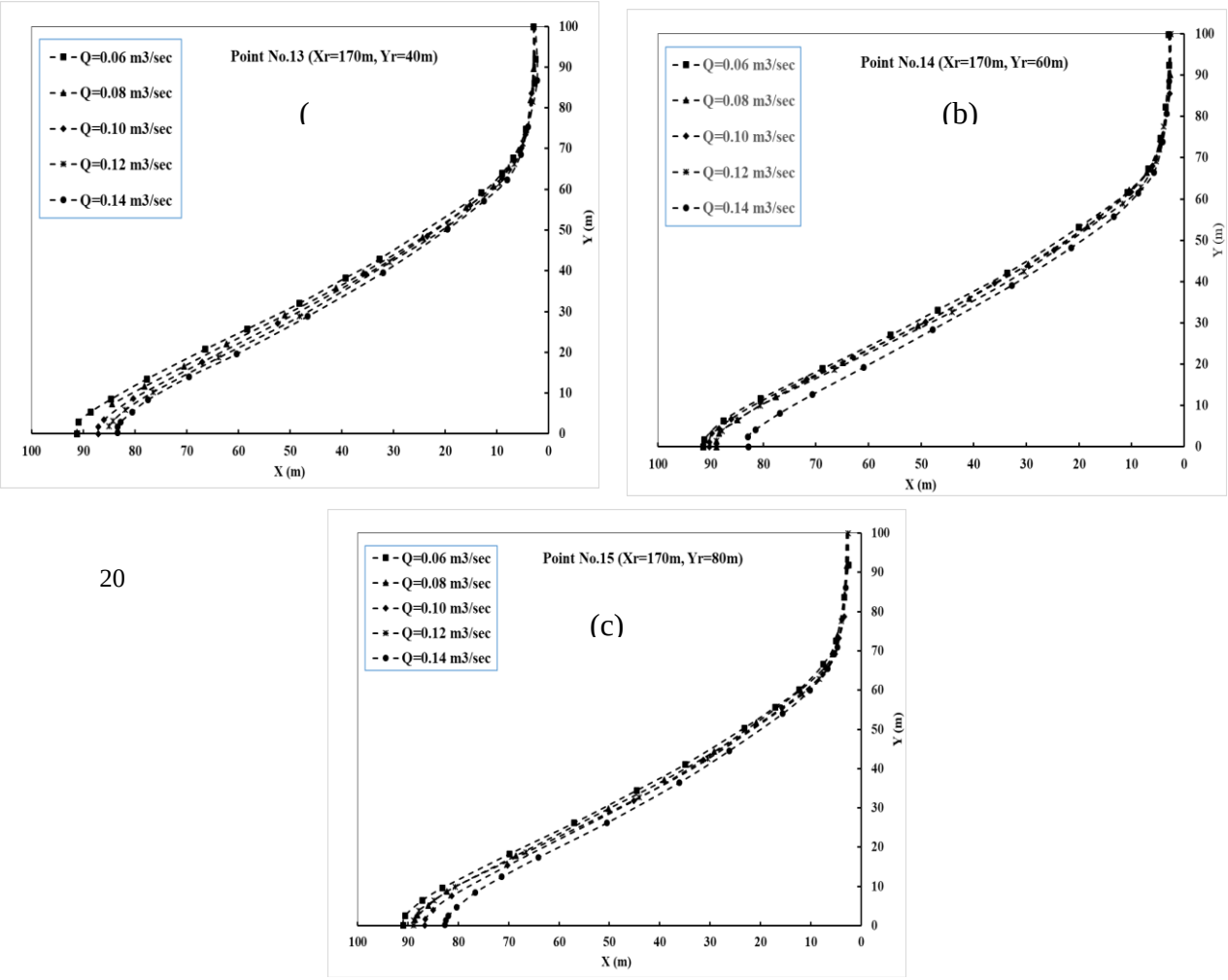

Figure .13: Saltwater intrusion wedge for five different recharge rates for points number:(a) 13,

Conclusion

The current research investigated the impact of using artificial recharge wells as a countermeasure to control the advancement of saltwater intrusion in unconfined coastal aquifer. The dimension of Henry saltwater problem was used to present the unconfined aquifer. The SEAWAT code was utilized to simulate the seawater intrusion in coastal aquifer. Sensitivity analysis was performed to check the impact of artificial recharge rate, well depth and well distance. For model calibration, the semi analytical solution of Henry problem was compared to the SEAWAT code solution of the current research. The points of freshwater injection located outside the sweater intrusion wedge. The results confirmed that increasing the artificial recharge rate forced the seawater intrusion wedge to attenuate back to the saltwater side. The minimum achieved repulsion ratio was observed at point 1 far away from the seawater wedge toe equals 5.8% for artificial recharge rate equals 0.06 m^3/sec. In addition, the maximum achieved repulsion ratio equals 18.2% at point 7 for artificial recharge rate equals 0.14 m^3/sec. Injection freshwater through wells at points close to the sweater wedge toe achieved highest repulsion ratio. On the other hand, injection of freshwater at points located far away from the saltwater wedge toe achieved the lowest values of repulsion ratio. The results of this research confirmed that artificial recharge through wells has a significant impact to control seawater intrusion in coastal aquifers. Artificial groundwater recharge is recommended as promising technique for controlling seawater intrusion in coastal aquifer and for groundwater management and development future projects.

References

1. Abdalla, O. E., & Al-Rawahi, A. (2013). Groundwater recharge dams in arid areas as tools for aquifer replenishment and mitigating seawater intrusion: Example of AlKhod, Oman. Environ. Earth Sci. 69: 1951–1962.
2. Abd-Elhamid, H. F., & Abdelaty, I. (2017). Application of a new methodology (TRAD) to control seawater intrusion in the Nile Della

Aquifer, Egypt. In: proceedings of the regional workshop, 25-30 April, Cairo, Egypt.

3. Abd-Elhamid, H. F., Abd-Elkader, B. S., Wahed, O., Zeleˇnáková, M., & Abd-Elaty, I. (2022). Assessment of Changing the Abstraction and Recharge Rates on the Land Subsidence in the Nile Delta, Egypt. Water 14: 1096. https://doi.org/10.3390/ w14071096
4. Abd-Elhamid, H. F., & Javadi, A. (2011). A cost-effective method to control seawater intrusion in coastal aquifers.Water Resour. Manag. 25: 2755–2780.
5. Allow, K. (2012). The use of injection wells and a subsurface barrier in the prevention of seawater intrusion: A modelling approach. Arab. J. Geosci. 5: 1151–1161.
6. Aziz, S. A., Zelenáková, M., Mésároš, P., Purcz, P., & Abd-Elhamid, H. F. (2019). Assessing the potential impacts of the Grand Ethiopian Renaissance Dam on water resources and soil salinity in the Nile Delta, Egypt. Sustainability, 11: 7050.
7. Barlow, P. M. (2000). Groundwater resources for the future: Atlantic coastal zone; US Geological Survey, US Department of the Interior: Washington, DC, USA.
8. El-Arabi N. (2012). Environmental management of groundwater in Egypt via artificial recharge extending the practice to Soil Aquifer Treatment (SAT)", International Journal of Environment and Sustainability, 1(3): 66-82.
9. Guo, W., & Langevin, C. D. (2002). User's guide to SEWAT: A computer program for simulation of three-dimensional variable-density groundwater flow. U.S. Geol. Surv., Reston, Va.
10. Hussain, M. S., Javadi, A. A., & Sherif, M. M. (2017). Assessment of different management scenarios to control seawater intrusion in unconfined coastal aquifers. J. Duhok Univ. 20: 259–275.
11. Huyakorn, P. S., Andersen, J. P. F., Mercer, J. W., & White, H. O. (1987). Saltwater intrusion in aquifers' development and Testing of a

three-dimensional finite element model. Water Resources Research, 23(2): 293-312.

12. IPCC, W. (2013). Working group I contribution to the IPCC fifth assessment report: climate change 2013: The physical science basis, summary for policymakers; IPCC: Cambridge, UK; New York, NY, USA.
13. Lu, C., Werner, A. D., Simmons, C.T., Robinson, N.I., & Luo, J. (2013). Maximizing net extraction using an injection-extraction well pair in a coastal aquifer. Groundwater, 51: 219–228.
14. Luyun, R., Momii, K., & Nakagawa, K. (2011). Effects of recharge wells and flow barriers on seawater intrusion. Ground Water, 49: 239–249.
15. Ma, J., Zhou, Z., Guo, Q., Zhu, S., Dai, Y., & Shen, Q. (2019). Spatial characterization of seawater intrusion in a coastal aquifer of northeast Liaodong Bay, China. Sustainability, 11: 7013.
16. Mahesha, A. (1996a). Transient effect of battery of injection wells on seawater intrusion. J. Hydraul. Eng. 122: 266–271.
17. Mahesha, A. (1996b). Steady-state effect of freshwater injection on seawater intrusion. J. Irrig. Drain. Eng. 122: 149–154.
18. Mahesha, A., & Nagaraja, S. H. (1996). Effect of natural recharge on sea water intrusion in coastal aquifers. J. Hydrol. 174: 211–220.
19. Narayan, K. A., Schleeberger, C., & Bristow, K. L. (2007). Modelling seawater intrusion in the Burdekin Delta irrigation area, north Queensland, Australia. Agric. Water Manag. 89: 217–228.
20. Narayan, K. A., Schleeberger, C., Charlesworth, P. B., & Bistrow, K. L. (2003). Effects of groundwater pumping on saltwater intrusion in the lower Burdekin Delta, North Queensland. In MODSIM 2003 International Congress on Modelling and Simulation; Post, D.A., Ed.; Modelling and Simulation Society of Australia and New Zealand, pp. 212–217.
21. Oude Essink, G. H. P. (2001). Improving fresh groundwater supply—problems and solutions. Ocean Coast. Manag. 44: 429–449.

22. Papadopoulou, M., Karatzas, G., Koukadaki, M., & Trichakis, Y. (2005). Modeling the saltwater intrusion phenomenon in coastal aquifers–A case study in the industrial zone of Herakleio in Crete. Glob. NEST J. 7: 197–203.
23. Paniconi, C., Khlaifi, I., Lecca, G., Giacomelli, A., & Tarhouni, J. A. (2001). Modelling study of seawater intrusion in the Korba coastal plain, Tunisia. Phys. Chem. Earth Part B Hydrol. Ocean. Atmos. 26: 345–351.
24. Paniconi, C., Khlaifi, I., Lecca, G., Giacomelli, A., & Tarhouni, J. (2001). Modeling and analysis of seawater intrusion in the coastal aquifer of eastern Cap-Bon, Tunisia. Transp. Porous Media, 43: 3–28.
25. Sebben, M. L., Werner, A. D., & Graf, T. (2015). Seawater intrusion in fractured coastal aquifers: A preliminary numerical investigation using a fractured Henry problem. Adv. Water Resour. 85: 93–108.
26. Sun, D. M., & Semprich, S. (2013). Using compressed air injection to control seawater intrusion in a confined coastal aquifer. Transp. Porous Media, 100: 259–278.
27. Todd, D. K. (1959). Groundwater hydrology; John Wiley & Sons: New York, NY, USA, p. 525.
28. Van Dam, J. C. (1999). Exploitation, restoration and management. In seawater intrusion in coastal aquifers- concepts, methods and practices; Kluwer Academic Publishers: Dordrecht, The Netherlands, pp. 7–125.
29. Yuansheng P, & Zhaohui T. (2009). Integrated project management of sustainable water storage and seawater intrusion prevention in a costal city. IEEE. 263−267.

دراسة عددية لتأثير التغذية الاصطناعية من خلال الآبار للتحكم في تسرب مياه البحر إلى طبقات المياه الجوفية الساحلية

فيليب يوسف كريم موسي [١] و اسعد مطر ارمانيوس [٢] و نهي سمير دنيا [٣] و سماح محمود مرسي [٤]

١)الهيئة المصرية العامة لمشروعات الصرف ، وزارة الموارد المائية والري ، مصر - طالب دارسات عليا، كلية الدراسات العليا والبحوث البيئية، جامعة عين شمس ، مصر .
٢)قسم هنسة الري والهيدروليكا ، كلية الهندسة ، جامعة طنطا، مصر ٣)كلية الدراسات العليا والبحوث البيئية، جامعة عين شمس، مصر ٤)كلية العلوم، جامعة عين شمس، مصر

المستخلص

يعتمد تطوير المناطق الساحلية إلى حد كبير على نظام المياه الجوفية ، وهو المصدر الأساسي للمياه العذبة في هذه المناطق. يعد تداخل المياه المالحة (SWI) في طبقات المياه الجوفية الساحلية للمياه العذبة مصدر قلق بيئي واسع النطاق يتسبب في تدهور جودة المياه الجوفية. تبحث هذه الدراسة في تأثير استخدام التغذية الاصطناعية من خلال آبار المياه الجوفية للتحكم في تسرب المياه المالحة إلى طبقات المياه الجوفية الساحلية غير المحصورة. تم استخدام كود SEAWAT للتحقيق في تأثير حقن المياه العذبة من خلال آبار المياه الجوفية للتحكم في تسرب المياه المالحة إلى طبقات المياه الجوفية الساحلية. تم استخدام التحليل شبه التحليلي لتداخل مياه البحر ومقارنة النتائج بحل برنامج SEAWAT للتحقق من النموذج. تم اختبار التغذية الاصطناعية لأعماق مختلفة من بئر المياه الجوفية ، والمسافات من خط شاطيء البحر ، ومعدل التغذية الاصطناعية. نقاط التغذية الاصطناعية الموجودة خارج مساحة تسرب المياه المالحة. أكدت النتائج أن حقن المياه العذبة بالقرب من نقطة مقدمة تسرب مياه البحر حقق نسبة تراجع أعلى. بلغت نسبة التراجع القصوى لتسرب مياه البحر ١٨.٢٪ والتي تم تحقيقها عند النقطة ٧ ، والتي كانت نقطة الحقن للابارقريبة من نقطة مقدمة تداخل مياه البحر وذلك بمعدل حقن قيمته ٠.١٤ م ٣ / ثانية. حقق حقن المياه العذبة عند النقاط ٧ و ١١ و ١٥ أعلى نسبة تراجع لقيم مختلفة لمعدلات الحقن. الحد الأدنى لنسبة التراجع المحققة لتداخل المياه المالحه يساوي ٥.٨٪ ، لوحظ عند النقطة ١ ، والتي تقع بعيدا عن نقطة مقدمة تداخل مياه البحر المالحة. يمكن استخدام نتائج هذا البحث لإدارة المياه العذبة في أنظمة المياه الجوفية في طبقات المياه الجوفية الساحلية.

الكلمات المفتاحية: تداخل مياه البحر، التغذية الاصطناعية، نسبة التراجع، خزان المياه الجوفية، نمذجة المياه الجوفية